A Novel Fiber-Based Variable All-Optical Packet Buffer Based on Self-Phase-Modulation-Induced Spectral Broadening

Kam-Hon Tse, *Student Member, IEEE*, and Chun-Kit Chan, *Senior Member, IEEE*

***Abstract*—We propose a novel optical delay control mechanism to realize variable all-optical packet buffering, in which the amount of optical delay is controlled by the input signal power level. It consists of a passive fiber delay loop followed by an optical power dependent filter, which is realized by means of two stages of self-phase-modulation-induced spectral broadening and offset filtering. The feasibility of the proposed optical packet buffer has been investigated through numerical simulations and experiments. No polarization control and additional laser source are needed.**

***Index Terms*—Fibers, fiber optics communications, nonlinear optics.**

I. Introduction

IN FUTURE optical packet switching (OPS) systems, data buffering is essential to resolve possible packet contention and it is considered as one of the greatest challenges in optical implementation. Although electronic buffer technology has been greatly improved recently, optical buffering is still an ideal candidate for future ultrahigh-speed transparent optical networks, as it does not require optical-electrical-optical (O-E-O) conversion and supports ultrafast data rates. In addition to data rate transparency, the absence of O-E-O conversion leads to much better power saving and reduced implementation cost. There are different categories of optical delay lines, including continuously tunable ones or discretely variable ones. They have found applications in optical coherence tomography, optical control of phased array antennas for radio frequency communication, bit-level synchronization for interleaving, demultiplexing, and switching, tapped delay lines for equalization, filtering, and chromatic dispersion compensation, etc. Nevertheless, the possible data packet buffering required for contention resolution in OPS systems might require relatively long fiber or an expensive wavelength converter with large tunable wavelength range, when it was implemented by wavelength conversion followed by a dispersive medium with group velocity dispersion [1], [2]. One interesting example is to convert the wavelength of the incoming data packet before being fed into a wavelength dependent delay element, where the signals at different wavelengths would experience different amount of temporal delays [3]. Another kind of optical delay lines was based on slow light induced by stimulated Brillouin scattering [4], [5]. Nevertheless, their applications might be limited by the small amount of induced delay and the possible severe signal degradation at increased delay values.

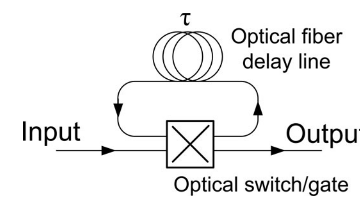

Fig. 1. Structure of an optical recirculating delay loop.

Fig. 1 shows a common way to implement optical buffers based on an optical recirculating loop, which required all-optical switches [6], optical switching via semiconductor optical amplifiers (SOAs) [7], [8], or through nonlinear polarization rotation inside the SOA [9], to control the number of circulations for the optical packet. However, it required synchronization between the switching time and the cycle of the packet propagation. In [10], an optical recirculating loop with an optical thresholding function was used to control the propagation of low-priority signal inside the loop, via wavelength conversion, so as to resolve the contention. In [11], the signal's wavelength was shifted by a certain amount after each cycle of circulation in an optical recirculating loop; thus, the output wavelength could be varied and controlled. In this paper, we propose an all-fiber variable optical packet buffer, in which the amount of delay is controlled by the input signal power level. The delay control is based on self-cloning the input optical signal, followed by optical power dependent filtering. The suggested optical subsystem implementation comprises a passive optical delay loop circuit and two stages of self-phase modulation (SPM) in highly nonlinear fiber (HNLF), followed by offset filtering. Due to the intrinsic nature of SPM, it does not require polarization control and no additional laser source is required.

This paper is organized as follows. Section II illustrates the proposed optical delay control mechanism for the variable optical packet buffer. Its operation principle and a feasible optical implementation will be discussed. Sections III and IV present the numerical simulation results as well as the experimental demonstration, respectively. Section V provides some discussions on the proposed optical packet buffer structure. Finally, Section VI summarizes this paper.

Manuscript received November 13, 2010; revised February 22, 2011; accepted March 16, 2011. Date of publication April 29, 2011; date of current version March 2, 2012.

The authors are with the Department of Information Engineering, The Chinese University of Hong Kong, Shatin, N. T., Hong Kong (e-mail: tkh008@ie.cuhk.edu.hk; ckchan@ie.cuhk.edu.hk).

Color versions of one or more of the figures in this paper are available online at http://ieeexplore.ieee.org.

Digital Object Identifier 10.1109/JSTQE.2011.2135336

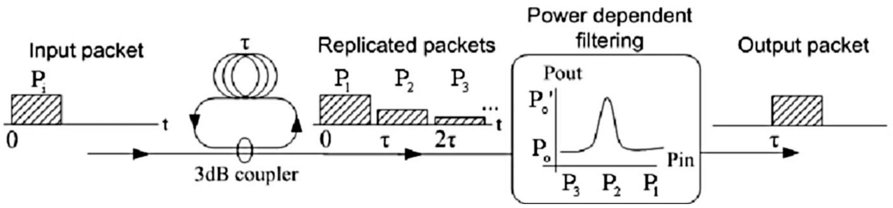

Fig. 2. Illustration on the delay control mechanism of the proposed optical packet buffer structure.

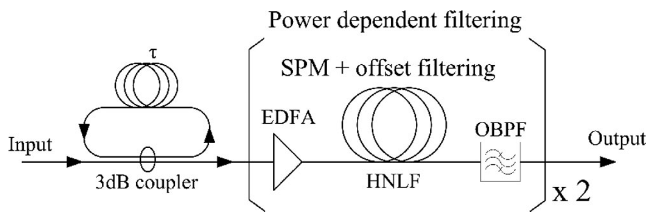

Fig. 3. Optical implementation of the proposed optical buffer.

II. Input Signal Power Dependent Delay

Having considered the pros and cons of the previously reported schemes for the implementations of variable optical buffer, we propose a novel all-fiber variable optical packet buffer architecture, which is based on a passive optical delay loop to provide long and discretely variable optical delay. The amount of optical delay induced is varied by controlling the input signal power level. Hence, simple optical data packet buffering in an OPS system can be realized.

Fig. 2 illustrates the principle of the delay control technique for the proposed optical packet buffer. The incoming optical packet with power P_i, first passes through a passive optical delay loop circuit to generate copies of the packets, temporally spaced by a fixed time interval τ. The power of each delayed packet copy is designed to be 3 dB lower than its previous one, and this is to create a mapping between different time delays and different input signal power levels. Therefore, optical packets having powers at P_1, P_2, P_3, ... , will appear at time instances of 0, τ, $2\tau, \ldots$, respectively, as illustrated in Fig. 2. As a 3-dB power coupler is employed, $P_2 = P_1/2$, $P_3 = P_1/4$, and so on. The generated optical packet train then undergoes optical power-dependent filtering operation. As a result, only the optical packet copy at the specified power level (e. g., P_2) with the desired respective time delay (e. g., τ) remains at the output, while other packet copies are dropped or suppressed. The optical power-dependent filter should be designed to have good power contrast between the transmission peak and floor, that is $P_o' \gg P_o$, as in Fig. 2, so as to achieve good extinction ratio in the output signal. Hence, such optical subsystem transforms different input signal power levels into different amount of time delays. The control of the time delay is achieved by altering the input signal power P_i such that the packet copy with the desired time delay and optical power level falls into the passband of the optical power dependent filter. Increasing the input signal power by 3 dB effectively induces an additional delay of τ. Ideally, the optical power of the output packet should be the same while the amount of delay varies.

Fig. 3 depicts a feasible implementation of the proposed optical packet buffer. It comprises a passive optical delay loop circuit, as described earlier, and an optical power-dependent filter, where two stages of SPM in HNLF with offset filtering are employed. The technique of employing SPM in HNLF with offset filtering has been widely studied in optical 2R signal regeneration [12]–[15] and was recognized as Mamyshev regenerator. It offers simple structure to perform noise suppression at zero level, in addition to amplitude equalization.

The input optical data packets are assumed to be modulated in return-to-zero pulsed format. In the first stage of SPM and offset filtering, spectral broadening of the optical pulses induced by SPM in HNLF creates multiple lobes in the spectrum [16], where the outermost lobes, located farther away from the center wavelength, contribute to higher signal power. In addition, the width of the broadened spectrum is increased with the input signal power. Any further increase in input signal power would lead to supercontinuum generation, where the output signal power is dispersed across a wide wavelength range. By optimal setting of the optical bandpass filter (OBPF) so as to filter out the outermost spectral lobes of the signal at the specified input signal power, only the optical packet copy with pulses at the same specified power level and the respective desired time delay remains at the output, while other packet copies are dropped or suppressed. Thus, the input signal power-dependent filtering operation is realized. The second stage of SPM and offset filtering performs optical power thresholding function so as to further enhance the extinction ratio between the output packet and the dropped packet copies.

III. Numerical Simulation Studies

In this section, the feasibility of this scheme has been investigated and characterized through numerical simulations. The simulation setup is shown in Fig. 4. The output from a 10-GHz mode-locked laser with 2.5-ps pulse width at 1547.38 nm was first modulated by an optical intensity modulator, generating an input optical packet with 20-bit pulse pattern. Then, it was fed into a passive optical power splitter connected with different fiber delay lines and attenuation values in order to simulate the output of the passive delay loop circuit, in the form of multiple copies of the input signal. Each subsequent delayed copy experienced an additional time delay of 3.5 ns and its power was relatively reduced by 3 dB, accordingly. The generated packet train then passed through two stages of SPM in HNLF and offset filtering to perform optical power-dependent filtering and power thresholding operations. In the first stage, a piece of 1-km dispersion-flattened highly nonlinear fiber

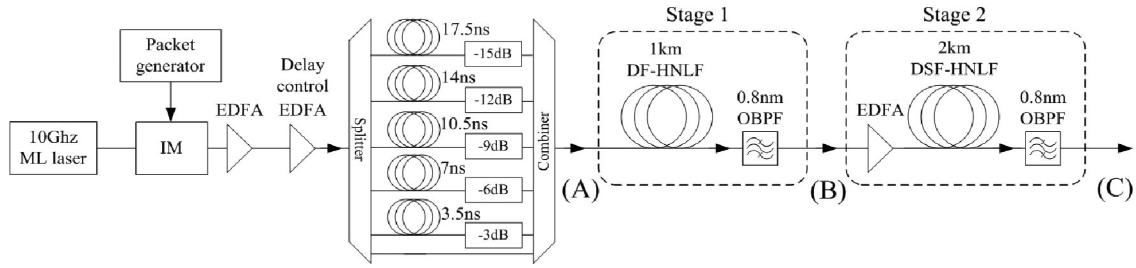

Fig. 4. Simulation setup (ML laser: mode-locked laser, IM: intensity modulator, OBPF: optical band pass filter).

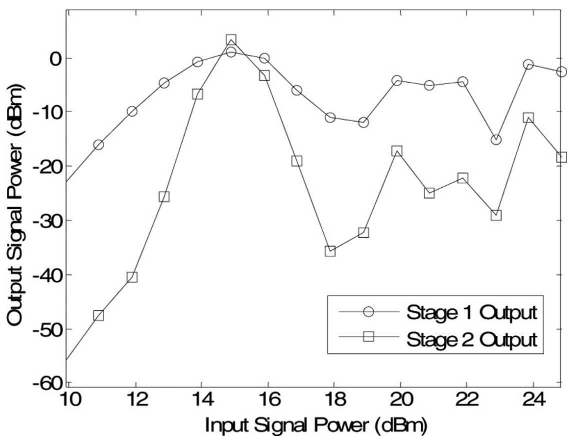

Fig. 5. Simulated power transfer curves of Stage 1 output and Stage 2 output of the proposed optical packet buffer.

(DF-HNLF) was used as the nonlinear medium and its nonlinear coefficient, zero-dispersion wavelength, and dispersion slope were 10.8 $W^{-1}\cdot km^{-1}$, 1550 nm, and 0.007 ps/($nm^2\cdot$km), respectively. The spectrally broadened signal was then filtered at 1541 nm, via a 0.8-nm bandwidth OBPF to realize power-dependent filtering. After being amplified via an erbium-doped fiber amplifier (EDFA), the output signal was then fed into the second stage of SPM and offset filtering to perform power thresholding. In this stage, a piece of 2-km dispersion-shifted-HNLF was employed and its nonlinear coefficient, zero dispersion wavelength, and dispersion slope were 11.9 $W^{-1}\cdot km^{-1}$, 1544 nm, and 0.018 ps/($nm^2\cdot$km), respectively. The output signal is then filtered by another 0.8-nm OBPF at the wavelength of 1535.5 nm.

First, the power transfer characteristics of the proposed optical packet buffer were studied using an unmodulated optical pulse train, as the input signal. Fig. 5 shows the output power of the two stages of SPM followed by offset filtering when optical pulses at different power levels were inputted to the proposed optical packet buffer. The power filtering effect was observed at the Stage 1 output (measured at point B in Fig. 4), which exhibited a maximum output when the input signal power was at about 15 dBm, while power thresholding operation was observed at the Stage 2 output (measured at point C in Fig. 4), which further enhanced the power contrast between the peak output power and its adjacent power trough in the power transfer curve. Fig. 6 shows the optical spectra measured at the output of Stage 1 at different input signal power levels, where the input power level was subsequently increased by 3 dB, so as to realize the same condition as in the multiple delayed copies at the output of the passive optical delay loop circuit. The insets in Fig. 6 show the enlarged diagram of the respective optical spectra. At low-input signal power, more power was observed to be concentrated at the outer spectral sidelobes, while at high-input

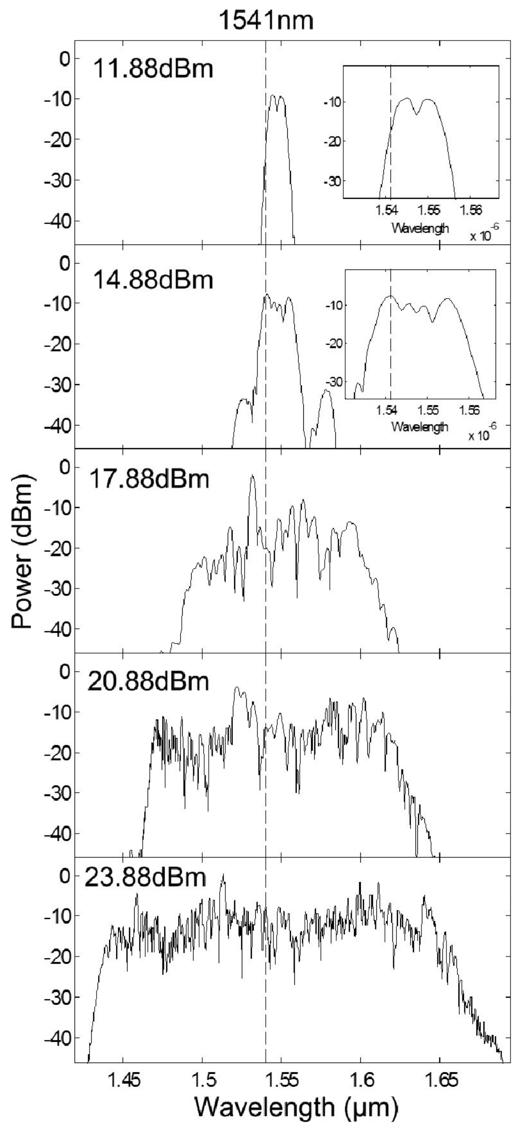

Fig. 6. Simulated optical spectra of the input pulse train at the output of Stage 1 with different input signal power levels into the HNLF.

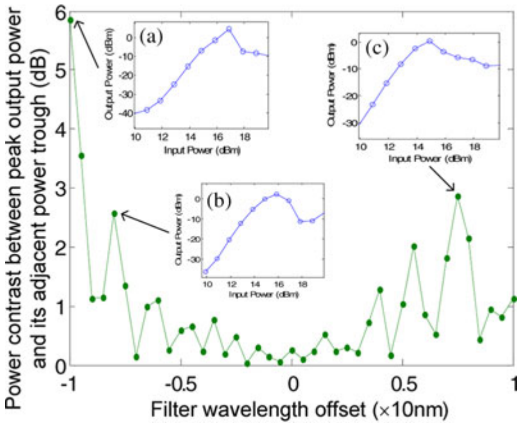

Fig. 7. Simulated power contrast between the peak output power and its adjacent power trough of Stage 1 outputs with different filter wavelength offset values with respect to the input signal wavelength. The insets show the power transfer curves when the filter wavelength offsets were set at (a) -10 nm, (b) -8 nm, and (c) $+7.5$ nm, respectively.

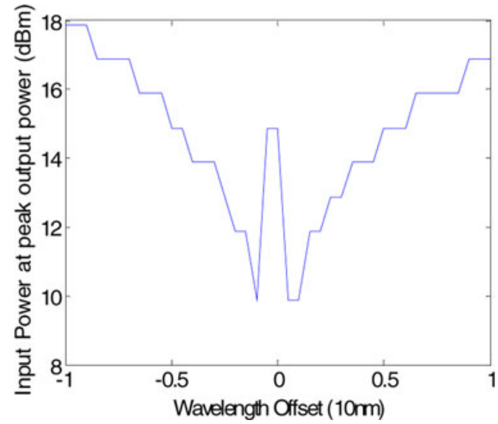

Fig. 8. Required input signal power of Stage 1 at peak output power with different filter wavelength offset values.

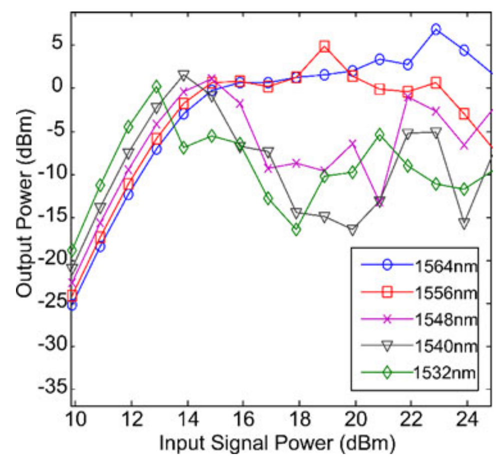

Fig. 9. Simulated power transfer curves at Stage 1 output for HNLFs with different HNLF zero-dispersion wavelengths, given that the input signal wavelength is 1547 nm.

signal power, supercontinuum generation occurred. The position of the offset filter at Stage 1 output was marked as the dotted line (at 1541 nm) in Fig. 6. When the input pulse train was at the optimum power, say 14.88 dBm, for example, one of the outer spectral sidelobes fell into the passband of the offset filter and thus its filter output gave a maximum power level. The other input pulse trains having lower input power levels did not get sufficient spectral broadening from SPM; thus, their filter outputs were at very low power level.

On the other hand, the input pulse train with power higher than the optimum level would give low power at the filter output, since the excess power had led to subsequent spectral broadening induced by the mixed effects of SPM, four-wave-mixing (FWM), and stimulated Raman scattering, and thus resulted in supercontinuum generation. Hence, the power of the input signal would get dispersed across a wide wavelength range and led to lower power level at filter output.

Fig. 7 shows the simulated power contrast between the peak output power and its adjacent power trough at Stage 1 output when the filter wavelength offset was varied from $+10$ to -10 nm, with respect to the input signal wavelength. The insets in Fig. 7 further show the power transfer curves at different filter wavelength offset values at (a) -10 nm, (b) -8 nm, and (c) 7.5 nm. The results show that such power contrast in the power transfer curve at Stage 1 output increased with the filter wavelength offset value. Although higher power contrast in the power transfer curve was more desirable for more effective power-dependent filtering, the respective input signal power required to achieve the respective peak output power was found to be increasing with the filter wavelength offset value, as illustrated in Fig. 8. Hence, there existed a tradeoff between the power contrast and the required input signal power in the power transfer curve at Stage 1 output.

Besides, the effect of the zero-dispersion wavelength of the HNLF employed in Stage 1 also imposed significant impact to the performance of the power-dependent filtering operation. Fig. 9 depicts the power transfer curve at Stage 1 output when the zero-dispersion wavelength of the HNLF employed was varied from 1532 to 1564 nm, given that the input signal wavelength was chosen at 1547 nm. It is shown that when the input signal wavelength was set in the anomalous dispersion regime (HNLF zero-dispersion wavelengths at 1532 and 1540 nm), the power filtering effect was quite prominent with good power contrast within a narrow input power range in the power transfer curve. This could be attributed to the fact that the signal peak power would reach a higher level, due to the pulse compression effect in the anomalous dispersion regime, and thus could help to foster the power-dependent filtering with better power contrast. However, due to the possible coherence degradation of the output signal when being operated in the anomalous dispersion regime [17]–[19], we had better operate the input signal in the normal dispersion regime, which corresponded to the power transfer curves with their respective HNLF zero-dispersion wavelengths at 1548, 1556, and 1564 nm, in Fig. 9. However, it is shown that the corresponding power-dependent filtering effect was much weakened and exhibited a plateau pattern over a much broader power range, as the input signal wavelength was set farther away from the zero-dispersion

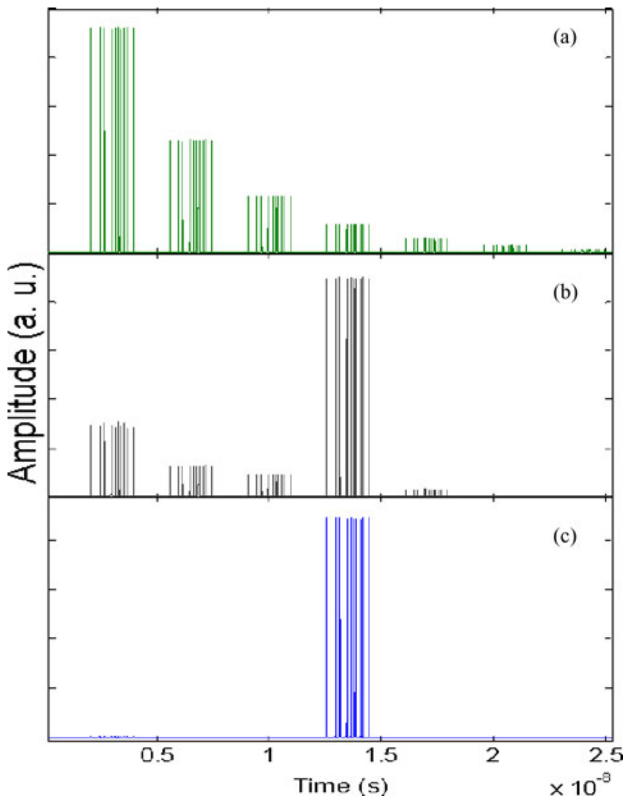

Fig. 10. Simulated outputs when the delay is controlled as three steps from its initial timing position. (a) Input packet train copies, (b) output from Stage 1, and (c) output from Stage 2.

wavelength value. The first power trough appeared at a much higher input signal power value. This might be attributed to the pulse broadening effect of the input signal in this normal dispersion regime and had led to reduced peak power of the input signal. Thus, the SPM effect was much weakened. To alleviate this, input signal pulses with much narrower pulse width might be required. As a result, the input signal wavelength value should be chosen not too far away from the zero-dispersion wavelength in the normal dispersion regime [20] to assure signal coherence as well as better power contrast in the power-dependent filtering operation.

Fig. 10(a)–(c) shows the packet copies of the input signal, and the output signals of Stages 1 and 2, respectively, when the input signal pulse was delayed by three steps from its initial position. Fig. 11 shows the output signals of the optical packet buffer when the input signal pulses with different power levels were inputted. It is observed that the output pulse was delayed by one further step when the input signal power was subsequently amplified by every 3 dB more, via the delay control EDFA, in the setup. The input signal power at its initial timing position was taken as 0-dB gain at the EDFA, as a reference.

IV. Experimental Results

The proof-of-concept of the proposed optical packet buffer has been experimentally investigated with the setup depicted in Fig. 12. The output of the semiconductor mode-locked laser at 1544.94 nm with 10-GHz 2-ps pulse train was modulated by

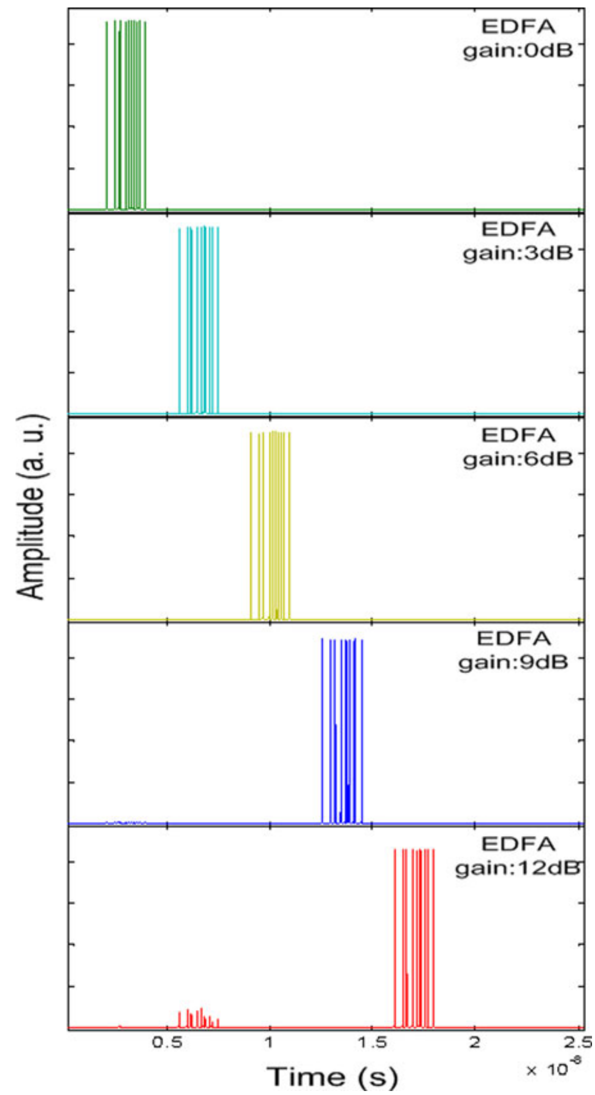

Fig. 11. Simulated outputs of optical packet buffer when the input signal is having different EDFA gains, which give different input signal power levels.

an optical intensity modulator to gate an optical pulse for every 64 pulses. The output of the intensity modulator was then amplified by an EDFA before being fed into the passive optical circuit formed by a 3-dB coupler which introduced 2-ns delay difference, and 3-dB power difference between each consecutive copy. The signal was then fed into the first stage of SPM followed by offset filtering that was made up of a piece of 1-km DF-HNLF, having a nonlinear coefficient, zero dispersion wavelength, and dispersion slope of 10.8 $W^{-1}\cdot km^{-1}$, 1550 nm, and 0.007 ps/($nm^2\cdot$km), respectively. The parameters were the same as those adopted in the numerical simulation in Section III. At the output of the HNLF, a 0.8-nm bandwidth OBPF centered at 1541 nm was used to slice the spectrally broadened signal. The spectrally sliced signal was then amplified before being fed into another piece of 4-km dispersion-shifted fiber (DSF) for power thresholding operation. At the output of the DSF, the signal was finally filtered out by another 0.8-nm OBPF at 1535.5 nm and was detected by a 50-GHz photodetector, followed by an

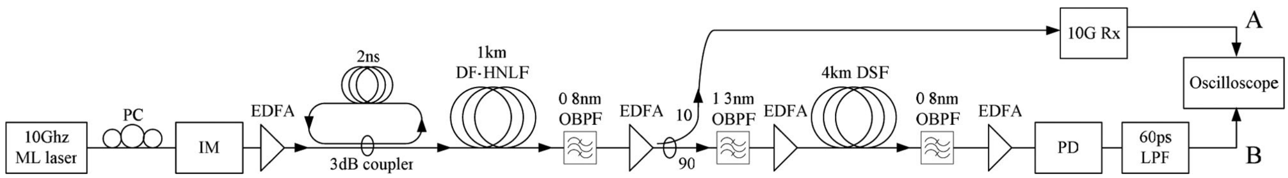

Fig. 12. Experimental setup (PD: photodiode, LPF: low-pass filter).

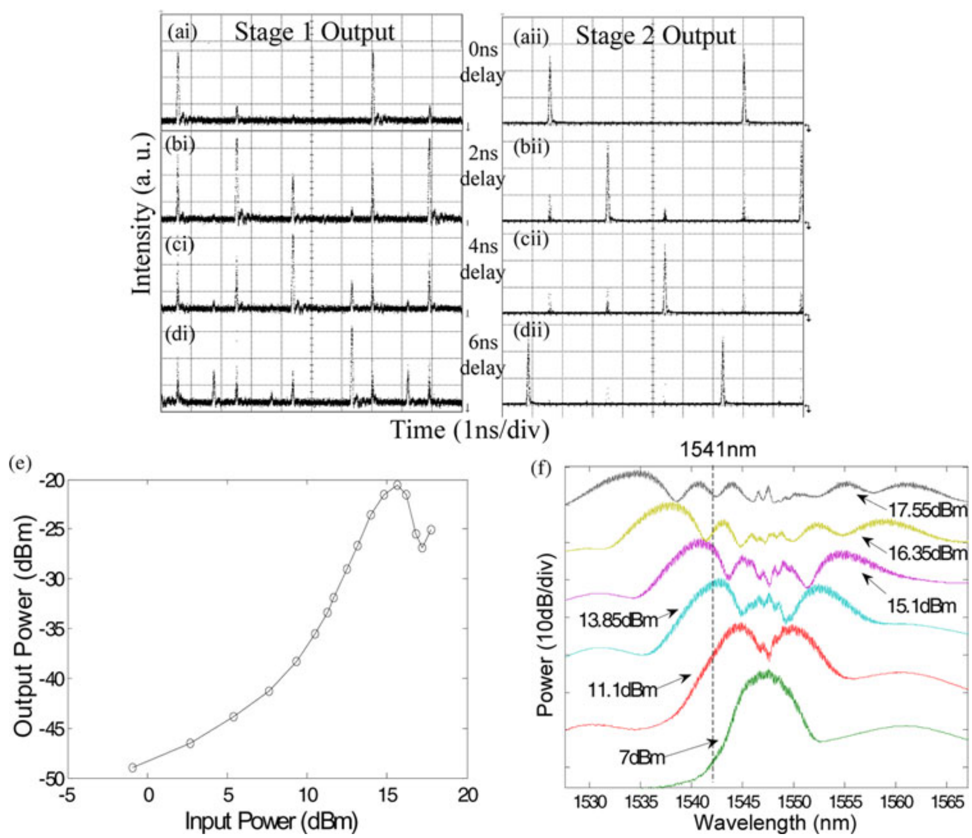

Fig. 13. (ai to di) Stage 1 output at point A in Fig. 12, (aii to dii) Stage 2 output at point B in Fig. 12 with different input signal power levels at Stage 1: (a) 0.4 dBm, (b) 3.85 dBm, (c) 6.25 dBm, (d) 8.75 dBm. (e) Power transfer curve of Stage 1 output. (f) Spectra evolution of the output pulse train at Stage 1 with different input power levels to the nonlinear fiber. (The spectra are arranged in the graph to avoid overlapping and the dotted line denotes the filter offset position at wavelength 1541 nm.)

electrical low-pass filter, in order to observe the delayed waveforms on the oscilloscope. Fig. 13(a)–(d) shows the outputs of the two stages when the input signal power level was varied. At the output of Stage 2, it was observed that the output signal was delayed by 0, 2, 4, and 6 ns, when their respective input signal power levels were 0.4, 3.85, 6.25, and 8.75 dBm, in which the power difference between each consecutive delay was roughly 3 dB. The Stage 1 output showed the signal extinction ratio of about 3 dB while the Stage 2 output showed the improvement of the signal extinction ratio after power thresholding operation. The results confirm the proof-of-concept of the proposed optical packet buffer, though the experimental results can be further improved by using HNLF of higher nonlinear coefficient to enhance the SPM effect, as well as optimizing the system parameters, such as pulse width, wavelength, and power of the input signal. Fig. 13(e) shows the power transfer curve at Stage 1, showing the power-dependent filtering phenomenon. Fig. 13(f) shows the measured spectral evolution of the output pulse train at Stage 1 at different input signal power levels to the HNLF. When starting at low-input power level, say 7 dBm, the output spectrum comprised only one spectral lobe centering at the input wavelength. Increasing the input signal power to 11.1 dBm would give rise to two spectral lobes in the spectrally broadened signal. Further increase in input power level to 13.85 dBm would form three spectral lobes in the spectrally broadened signal, and so on. Therefore, the spectral broadening increases when input signal power is increased.

More importantly, it was observed that the outermost spectral sidelobes contained more power than the inner spectral lobes. The asymmetry of the broadened spectrum was attributed to the fiber chromatic dispersion. By setting the filter wavelength offset at 1541 nm, denoted as the dotted line in Fig. 13(f), it was observed that the outermost spectral sidelobe fell into the passband of the offset filter when the input signal pulse stream was at 15.1 dBm and the outermost sidelobes were spreaded over wider wavelength range at higher input signal power level.

Fig. 13(e) shows the measured power transfer curve at the output of Stage 1 where the offset filter was centered at 1541 nm. The result confirmed that there was maximum output power when the input signal power was around 15 dBm.

V. Discussion

The optical power-dependent filter of the proposed variable optical packet buffer can be implemented via two stages of SPM followed by offset filtering. The first stage extracts the outermost spectral sidelobe at the desired input signal power while the second stage performs power thresholding operation to further enhance the extinction ratio of the signal output. In addition to easy control of the delay by controlling the input signal power level, this scheme offers two features that are intrinsic to the SPM effect, namely polarization independent and no additional laser source required. Besides, this scheme is potentially capable of supporting much higher bit rates.

From the numerically simulated power transfer curve of the Stage 2 output of the proposed optical packet buffer, as depicted in Fig. 5, the output power was maximized when the input signal power level was about 15 dBm. Any 2-dB difference from this optimum input signal power level would lead to at least 20-dB reduction in the output power with respect to the maximum output power level. Therefore, the design of the proposed optical buffer can be further optimized in such a way that the power of each subsequent delayed packet copy from the passive optical delay loop circuit is 2 dB lower than its previous one. As a result, the proposed optical packet buffer can provide a larger number of delay steps with smaller range of input power control.

The power requirement of the system can be lowered if highly nonlinear optical fiber with higher nonlinear coefficient is employed. Recently, due to the advance of the development of highly nonlinear fiber, the nonlinear coefficient of the fiber can achieve beyond 1000 $W^{-1}\cdot km^{-1}$ by using highly nonlinear bismuth oxide fiber (Bi-NLF) [21] or photonic crystal fiber (PCF) [22]. As Bi-NLF and PCF can provide much higher nonlinear coefficient, the fiber length to be used inside the system can be much shortened, and the power requirement of the input signal can be much relaxed.

Regarding to the realization of the optical power-dependent filtering operation in Stage 1, there may be other feasible approaches. For example, when the input pulse width is in femtosecond range and soliton self-frequency shifting (SSFS) [23] is utilized, the red wavelength shifted signal at the desired input signal power can be filtered out. The principle is similar to the case of SPM followed by offset filtering, as the increase in the input signal power level would lead to the increase in the red shifted wavelength offset of the signal, via SSFS, and vice versa. By setting the output filter at a certain strategic wavelength, there would be output power only at the specified input signal power and therefore realizes optical power-dependent filtering operation. SSFS has been demonstrated to provide continuously tunable optical delay line [24], in which SSFS introduced input signal power-dependent wavelength shift and in turn induced different time delays when the signal passed through a dispersive medium. However, long length of dispersive medium might be required in order to obtain larger amount of time delay. Besides SSFS, triangular pulse or sawtooth pulse has been employed to perform all-optical wavelength conversion [25], [26]. Owing to the temporal profile of such special pulse shapes, through SPM or cross-phase modulation, the amount of wavelength shift would be intensity dependent, which thus can be a potential alternative approach to perform intensity-dependent filtering in our proposed optical packet buffer with careful setting of the output filter wavelength. The generation of the triangular pulses can be realized through superstructured fiber Bragg grating technology [26] or chirped pulses propagating in a piece of normally dispersive fiber [27]. Regarding to the realization of the second stage that performs power thresholding operation, besides employing the Mamyshev regenerator structure, extinction ratio improvement can also be achieved through FWM [28], nonlinear amplifying optical loop mirror [29], [30], saturable absorber [31], etc.

VI. Summary

We have proposed a novel all-fiber optical packet buffer in which the amount of induced time delay is easily controlled by changing the input signal power level. It is realized by employing a passive optical delay loop circuit, followed by two stages of SPM spectral broadening effect in HNLF with offset filtering. We have investigated and characterized the proposed variable all-optical packet buffer both numerically and experimentally. Packet delay is achieved that can help to resolve the packet contention in future OPS systems.

References

[1] J. E. Sharping, Y. Okawachi, J. van Howe, C. Xu, Y. Wang, A. E. Willner, and A. L. Gaeta, "All-optical, wavelength and bandwidth preserving, pulse delay based on parametric wavelength conversion and dispersion," *OSA Opt. Exp.*, vol. 13, no. 20, pp. 7872–7877, Oct. 2005.

[2] N. Alic, J. R. Windmiller, J. B. Coles, and S. Radic, "Two-pump parametric optical delays," *IEEE J. Sel. Topics Quantum Electron.*, vol. 14, no. 3, pp. 681–690, May/Jun. 2008.

[3] J. D. LeGrange, J. E. Simsarian, P. Bernasconi, L. Buhl, J. Gripp, and D. T. Neilson, "Demonstration of an integrated buffer for an all-optical packet router," *IEEE Photon. Technol. Lett.*, vol. 21, no. 12, pp. 781–783, Jun. 2009.

[4] Z. Zhu, A. M. C. Dawes, D. J. Gauthier, L. Zhang, and A. E. Willner, "Broadband SBS slow light in an optical fiber," *J. Lightw. Technol.*, vol. 25, no. 1, pp. 201–206, Jan. 2007.

[5] A. E. Willner, B. Zhang, L. Zhang, L. Yan, and I. Fazal, "Optical signal processing using tunable delay elements based on slow light," *IEEE J. Sel. Topics Quantum Electron.*, vol. 14, no. 3, pp. 691–705, May/Jun. 2008.

[6] A. M. Liu, C. Q. Wu, M. S. Lim, Y. D. Gong, and P. Shum, "Optical buffer configuration based on a 3×3 collinear fibre coupler," *IET Electron. Lett.*, vol. 40, no. 16, pp. 1017–1019, Aug. 2004.

[7] R. Langenhorst, M. Eiselt, W. Pieper, G. Grosskopf, R. Ludwig, L. Kuller, E. Dietrich, and H. G. Weber, "Fiber loop optical buffer," *J. Lightw. Technol.*, vol. 14, no. 3, pp. 324–335, Mar. 1996.

[8] E. F. Burmeister, J. P. Mack, H. N. Poulsen, B. Stamenic, M. Masanovic, D. J. Blumenthal, and J. E. Bowers, "Demonstration of contention resolution between two 40 Gb/s packet streams using multiple photonic chip optical buffers," presented at the European Conference on Optical Communication, Brussels, Belgium, 2008, Paper We.2.D.3.

[9] M. Cheng, C. Wu, J. Hiltunen, Y. Wang, Q. Wang, and R. Myllyla, "A variable delay optical buffer based on nonlinear polarization rotation in semiconductor optical amplifier," *IEEE Photon. Technol. Lett.*, vol. 21, no. 24, pp. 1885–1887, Dec. 2009.

[10] Y. Liu, M. T. Hill, R. Geldenhuys, N. Calabretta, H. de Waardt, G. D. Khoe, and H. J. S. Dorren, "Demonstration of a variable optical delay for a recirculating buffer by using all-optical signal processing," *IEEE Photon. Technol. Lett.*, vol. 16, no. 7, pp. 1748–1750, Jul. 2004.
[11] T. Sakamoto, K. Noguchi, R. Sato, A. Okada, Y. Sakai, and M. Matsuoka, "Variable optical delay circuit using wavelength converters," *IET Electron. Lett.*, vol. 31, no. 7, pp. 454–455, Mar. 2001.
[12] P. V. Mamyshev, "All-optical data regeneration based on self-phase modulation effect," in *Proc. Eur. Conf. Opt. Commun.*, Madrid, Spain, 1998, pp. 475–476.
[13] M. Matsumoto, Y. Shimada, and H. Sakaguchi, "Two-stage SPM-based all-optical 2R regeneration by bidirectional use of a highly nonlinear fiber," *IEEE J. Quantum Electron.*, vol. 45, no. 1, pp. 51–58, Jan. 2009.
[14] J. Fatome and C. Finot, "Scaling guidelines of a soliton-based power limiter for 2R-optical regeneration applications," *J. Lightw. Technol.*, vol. 28, no. 17, pp. 2552–2559, Sep. 2010.
[15] S. H. Chung, X. Tang, and J. C. Cartledge, "Performance of a polarization-insensitive all-optical 3R regenerator using cross- and self-phase modulation and offset filtering in a recirculating loop," presented at the Optical Fiber Communication Conference/National Fiber Optical Engineering Conference, San Diego, CA, 2009, Paper OThF2.
[16] G. P. Agrawal, *Nonlinear Fiber Optics*. New York: Academic, 2001.
[17] M. Nakazawa, H. Kubota, and K. Tamura, "Random evolution and coherence degradation of a high-order optical soliton train in the presence of noise," *OSA Opt. Lett.*, vol. 24, no. 5, pp. 318–320, Mar. 1999.
[18] Z. Yusoff, P. Petropoulos, K. Furusawa, T. M. Monro, and D. J. Richardson, "A 36-channel x 10-Ghz spectrally sliced pulse source based on supercontinuum generation in normally dispersive highly nonlinear holey fiber," *IEEE Photon. Technol. Lett.*, vol. 15, no. 12, pp. 1689–1691, Dec. 2003.
[19] M. Nakazawa, K. Tamura, H. Kubota, and E. Yoshida, "Coherence degradation in the process of supercontinuum generation in an optical fiber," *Opt. Fiber Technol.*, vol. 4, pp. 215–223, 1998.
[20] Y. Takushima, F. Futami, and K. Kikuchi, "Generation of over 140-nm-wide super-continuum from a normal dispersion fiber by using a mode-locked semiconductor laser source," *IEEE Photon. Technol. Lett.*, vol. 10, no. 11, pp. 1560–1562, Nov. 1998.
[21] M. P. Fok and C. Shu, "Recent advances in optical processing techniques using highly nonlinear bismuth oxide fiber," *IEEE. J. Sel. Topics Quantum Electron.*, vol. 14, no. 3, pp. 587–598, May/Jun. 2008.
[22] J. H. Lee, W. Belardi, K. Furusawa, P. Petropoulos, Z. Yusoff, T. M. Monro, and D. J. Richardson, "Four-wave mixing based, 10 Gbit/s tunable wavelength conversion using a holey fiber with a high SBS threshold," *IEEE Photon. Technol. Lett.*, vol. 15, no. 3, pp. 440–442, Mar. 2003.
[23] F. M. Mitschke and L. F. Mollenauer, "Discovery of the soliton self-frequency shift," *OSA Opt. Lett.*, vol. 11, no. 10, pp. 659–661, 1986.
[24] S. Oda and A. Maruta, "Experimental demonstration of all-optical tunable delay line based on soliton self-frequency shift and filtering supercontinuum spectrum," presented at the European Conference on Optical Communication, Cannes, France, 2006.
[25] A. I. Lakin, S. Boscolo, R. S. Bhamber, and S. K. Turitsyn, "Optical frequency conversion, pulse compression and signal copying using triangular pulses," presented at the European Conference on Optical Communication, Brussels, Belgium, 2008, Paper Mo.3. F.4.
[26] F. Parmigiani, M. lbsen, T. T. Ng, L. Provost, P. Petropoulos, and D. J. Richardson, "Efficient wavelength conversion using triangular pulses generated using a superstructured fiber Bragg grating," presented at the Optical Fiber Communication Conference/National Fiber Optical Engineering Conference, San Diego, CA, 2008, Paper OMP3.
[27] A. I. Latkin, S. Boscolo, and S. K. Turitsyn, "Passive nonlinear pulse shaping in normally dispersive fiber," presented at the Optical Fiber Communication Conference/National Fiber Optical Engineering Conference, San Diego, CA, 2008, Paper OTuB7.
[28] A. Argyris, H. Simos, A. Ikiades, E. Roditi, and D. Syvridis, "Extinction ratio improvement by four-wave mixing in dispersion- shifted fibre," *Electron. Lett.*, vol. 39, no. 2, pp. 230–232, Aug. 2003.
[29] A. G. Striegler and B. Schmauss, "Extinction ratio improvement by an advanced NOLM setup," *IEEE Photon. Technol. Lett.*, vol. 18, no. 9, pp. 1058–1060, May 2006.
[30] C. Stephan, K. Sponsel, G. Onishchukov, B. Schmauss, and G. Leuchs, "Phase-preserving amplitude regeneration in DPSK transmission systems using a nonlinear amplifying loop mirror," *IEEE J. Quantum Electron.*, vol. 45, no. 11, pp. 1336–1343, Nov. 2009.
[31] D. Massoubre, J. L. Oudar, J. Fatome, S. Pitois, G. Millot, J. Decobert, and J. Landreau, "All-optical extinction-ratio enhancement of a 160 GHz pulse train by a saturable-absorber vertical microcavity," *Opt. Lett.*, vol. 31, no. 4, pp. 537–539, Feb. 2006.

Kam-Hon Tse (S'09) received the B.Eng. degree in information engineering from The Chinese University of Hong Kong, Hong Kong, in 2008 where he is currently working toward the Ph.D. degree in the same department.

His research interests include high-speed all-optical signal processing and optical packet switching.

Chun-Kit Chan (S'93–M'97–SM'04) received the B.Eng., M.Phil., and Ph.D. degrees from The Chinese University of Hong Kong, Hong Kong, all in information engineering.

In 1997, he joined the Department of Electronic Engineering, City University of Hong Kong, as a Research Assistant Professor. In 1999, he joined Bell Laboratories, Lucent Technologies, Holmdel, NJ, as a Member of Technical Staff, where he was engaged in control of widely tunable semiconductor lasers and realization of an optical packet switch fabric with terabit-per-second capacity. In August 2001, he joined the Department of Information Engineering, The Chinese University of Hong Kong, where he is currently an Associate Professor. He has authored or coauthored more than 200 technical papers in refereed international journals and conference proceedings, has edited one book on optical performance monitoring, and two book chapters on passive optical networks. He holds one issued U. S. patent. His research interests include enabling technologies for optical metro/access networks, optical networking design, high-speed optical signal processing, and optical performance monitoring.

Dr. Chan was a member of the Technical Program Committee for Optical Fiber Communication Conference / National Fiber Optic Engineers Conference and a number of other international conferences. He was an Associate Editor of the Optical Society of America (OSA) *Journal of Optical Networking*, and IEEE/OSA JOURNAL OF OPTICAL COMMUNICATIONS AND NETWORKING.